INTERNATIONAL CONFERENCE ON LIGHTNING PROTECTION
33rd International Conference on Lightning Protection
25 - 30 September 2016
Estoril, Portugal

Lightning Electromagnetic Pulse Simulation Using 3D-FDTD Method

(*Comparison between PEC and UPLM Boundary Conditions*)

K. Arzag
Dept. of Electrotechnics
University of Saida.
Saida, Algeria
ar_kado2006@yahoo.fr

Z. Azzouz
Dept. of Automatic Control
USTO "MB"of Oran
Oran, Algeria
azzazzouz@yahoo.fr

B. Ghemri
Dept. of Electrotechnics
USTO "MB"of Oran
Oran, Algeria
ghemri_b@yahoo.fr

Abstract-**In this paper we present an extensive comparison between the uses of two formulations related to the finite differences time domain method in three dimensions (3D-FDTD) applied to the lightning electromagnetic pulses (LEMP) analysis. Electromagnetic models are implemented for the representation of the lightning return stroke current.**
Thus, the first formulation is based on the implementation of the Yee algorithm using perfect electric conductor (PEC) boundary conditions. The second formulation consists on the integration of Taflove formulation in the 3D-FDTD method using uniaxial perfectly matched layers (UPML) boundary conditions. For that effect, two computational electromagnetic codes have been developed, in Matlab programming environment, in order to determine the lightning return stroke current distribution and associated electromagnetic field components. Finally, for validation needs, the obtained simulation results, especially the lightning vertical electric field and the magnetic flux density, are compared with measured results taken from specialized literature.

Index terms—**Lightning**, **Electromagnetic models, LEMP, 3D-FDTD method, PEC, UPML.**

I. INTRODUCTION

Lightning electromagnetic radiation is one of the most important disturbance's sources that could cause large damages on electric systems notably the electrical surges. So to predict theses effects it is necessary to implement electromagnetic computation methods in order to analyze the return stroke current distribution along the lightning channel and the associated electromagnetic field components.

Furthermore, lightning return stroke current distribution models are classified by Rakov and Uman [1] into four classes: gas dynamic models, electromagnetic models, distributed circuit models, and "engineering" models. Electromagnetic models, based on Maxwell's equations, are suitable for analyzing the lightning current and the associated electromagnetic field. This class of models yield to solve Maxwell's equations to have a spatio-temporal distribution of the return stroke current along the lightning channel using numerical methods as the moment method (MoM) in time domain (Van Barcium and Mailler[2]), the moment method (MoM) in frequency domain (Harrington [3]) and the finite differences method in time domain (FDTD) (Yee [4]). The MoM method in time domain is used by Moini and *al*. [5] for having a numerical solution of the electric field integral equation; this allows us to predict the current stroke distribution along the lightning channel. Shoory and *al*. [6] employed the MoM method in frequency domain for a vertical resistive wire excited by a lumped current source in order to analyze the lightning current. The FDTD method was used by Baba and Rakov [7-8-9-10] for the specification of the time-space return stroke current distribution and for the associated electromagnetic field.

In addition, the development of the lightning return stroke and its associated electromagnetic field computation, based on the FDTD method, requires an adequate choice of the boundary conditions in order to avoid reflections phenomena occurring at all working space boundaries. In this context, we compare in this paper, two different formulations of 3D-FDTD method; the first one is based on Yee [4] algorithm using PEC (perfectly electric conductor) boundary conditions while the second one based on the implementation of Taflove [11] formulation combined to the use of UPML (uniaxial perfectly matched layer) boundary conditions.

The present work is structured as follow. In section one; we present a short introduction on the lightning return stroke current determination and the associated electromagnetic field. In section two we review the theoretical aspects of formulations and boundary conditions used in this study. Section three is devoted firstly to the lightning current modeling and secondly to the presentation and discussion of the obtained simulation results.

II. 3D-FDTD FORMULATIONS AND BOUNDARY CONDITIONS

a. Yee algorithm and PEC boundary conditions

According to Yee [4], The Electric and magnetic fields components are calculated by using the discretized Maxwell's equations as follow:

$$E_z^n\left(i,j,k+\frac{1}{2}\right)=\frac{1-\dfrac{\sigma\left(i,j,k+\frac{1}{2}\right)\Delta t}{2\varepsilon\left(i,j,k+\frac{1}{2}\right)}}{1+\dfrac{\sigma\left(i,j,k+\frac{1}{2}\right)\Delta t}{2\varepsilon\left(i,j,k+\frac{1}{2}\right)}}E_z^{n-1}\left(i,j,k+\frac{1}{2}\right)$$

$$+\frac{\dfrac{\Delta t}{\varepsilon\left(i,j,k+\frac{1}{2}\right)}}{1+\dfrac{\sigma\left(i,j,k+\frac{1}{2}\right)\Delta t}{2\varepsilon\left(i,j,k+\frac{1}{2}\right)}}.$$

$$\left[\frac{H_y^{n-1/2}\left(i+\frac{1}{2},j,k+\frac{1}{2}\right)-H_y^{n-1/2}\left(i-\frac{1}{2},j,k+\frac{1}{2}\right)}{\Delta x}\right.$$
$$\left.-\frac{H_x^{n-1/2}\left(i,j+\frac{1}{2},k+\frac{1}{2}\right)-H_x^{n-1/2}\left(i,j-\frac{1}{2},k+\frac{1}{2}\right)}{\Delta y}\right] \quad (1\text{-a})$$

$$H_y^{n+1/2}\left(i+\frac{1}{2},j,k+\frac{1}{2}\right)=H_y^{n-1/2}\left(i+\frac{1}{2},j,k+\frac{1}{2}\right)$$
$$-\frac{\Delta t}{\mu\left(i+\frac{1}{2},j,k+\frac{1}{2}\right)}.$$
$$\left[\frac{E_x^n\left(i+\frac{1}{2},j,k+1\right)-E_x^n\left(i+\frac{1}{2},j,k\right)}{\Delta z}\right.$$
$$\left.-\frac{E_z^n\left(i+1,j,k+\frac{1}{2}\right)-E_z^n\left(i,j,k+\frac{1}{2}\right)}{\Delta x}\right] \quad (1\text{-b})$$

Equation (1-a), based on Ampere's low, allows the updating of the electric field *z* component: $E_z(i,j,k+1/2)$, at point $x=i.\Delta x$, y$=j.\Delta y$ and $z=(k+1/2).\Delta z$, and at time $t=n.\Delta t$.

Equation (1-b), based on Faraday's low, allows the updating of the magnetic field *y* component: $Hy\ (i+1/2,j,k+1/2)$, at point $x=(i+1/2).\Delta x, y=j.\Delta y$ and $z=(k+1/2).\Delta z$, and at time t$=(n+1/2).\Delta t$.

Equation updating the electric field *x* and *y* component's and the magnetic field *x* and *z* component's can be written in the same manner.

Perfect electric conductor (PEC) boundary conditions are specified by simply setting the boundary electric fields to be equal to zero.

The FDTD method, based on Yee algorithm [11] and associated with perfectly matched layer (PML) based on the Berenger [13] formulation and the second order Lioas boundary conditions, was employed in 2D and 3D by Baba and Rakov in various works [7], [8], [9] and [10]. So, in this paper, we propose the implementation of Taflove formulation in the 3D-FDTD method based on lightning current electromagnetic model and using UPML boundary conditions. The aim of this new approach is to improve the quality of obtained results in order to reach measurement data as much as possible.

b. Taflove formulation of 3D-FDTD method and UPML boundary conditions

The Taflove formulation of 3D-FDTD method used, to analyze the lightning current and the associated electromagnetic field, in this work has the advantage that it allows us to calculate the electromagnetic components in the entire work space and setting a uniaxial perfectly matched layer (UPML) absorbing boundary conditions using the same equations of electric and magnetic field associated to their densities. This is obtained by employing a simple change into mediums parameters (working space medium and UPML regions).

Equations representing this formulation can be written as follow:

$$D_x^{n+1}\left(i+\frac{1}{2},j,k\right)=\left(\frac{2\varepsilon k_y-\sigma_y\Delta t}{2\varepsilon k_y+\sigma_y\Delta t}\right).D_x^n\left(i+\frac{1}{2},j,k\right)$$
$$+\left(\frac{2\varepsilon\Delta t}{2\varepsilon k_y+\sigma_y\Delta t}\right).$$
$$\left[\frac{H_z^{n+1/2}\left(i+\frac{1}{2},j+\frac{1}{2},k\right)-H_z^{n+1/2}\left(i+\frac{1}{2},j-\frac{1}{2},k\right)}{\Delta y}\right.$$
$$\left.-\frac{H_y^{n+1/2}\left(i+\frac{1}{2},j,k+\frac{1}{2}\right)-H_y^{n+1/2}\left(i+\frac{1}{2},j,k-\frac{1}{2}\right)}{\Delta z}\right] \quad (2\text{-a})$$

$$E_x^{n+1}\left(i+\frac{1}{2},j,k\right)=\left(\frac{2\varepsilon k_z-\sigma_z\Delta t}{2\varepsilon k_z+\sigma_z\Delta t}\right).E_x^n\left(i+\frac{1}{2},j,k\right)$$
$$+\left[\frac{1}{(2\varepsilon k_z+\sigma_z\Delta t)\varepsilon}\right].$$
$$\left[(2\varepsilon k_x+\sigma_x\Delta t).D_x^{n+1}\left(i+\frac{1}{2},j,k\right)\right.$$
$$\left.-(2\varepsilon k_x-\sigma_x\Delta t).D_x^n\left(i+\frac{1}{2},j,k\right)\right] \quad (2\text{-b})$$

$$B_x^{n+3/2}\left(i,j+\frac{1}{2},k+\frac{1}{2}\right)=$$
$$\left(\frac{2\varepsilon k_y-\sigma_y\Delta t}{2\varepsilon k_y+\sigma_y\Delta t}\right).B_x^{n+1/2}\left(i,j+\frac{1}{2},k+\frac{1}{2}\right)$$
$$+\left(\frac{2\varepsilon\Delta t}{2\varepsilon k_y+\sigma_y\Delta t}\right).$$
$$\left[\frac{E_z^{n+1}\left(i,j+1,k+\frac{1}{2}\right)-E_z^{n+1}\left(i,j,k+\frac{1}{2}\right)}{\Delta y}\right.$$
$$\left.-\frac{E_y^{n+1}\left(i,j+\frac{1}{2},k+1\right)-E_y^{n+1}\left(i,j+\frac{1}{2},k\right)}{\Delta z}\right] \quad (2\text{-c})$$

$$H_x^{n+3/2}\left(i,j+\frac{1}{2},k+\frac{1}{2}\right)=$$
$$\left(\frac{2\varepsilon k_z-\sigma_z\Delta t}{2\varepsilon k_z+\sigma_z\Delta t}\right).H_x^{n+1/2}\left(i,j+\frac{1}{2},k+\frac{1}{2}\right)$$
$$+\left[\frac{1}{(2\varepsilon k_z+\sigma_z\Delta t)\mu}\right].$$
$$\left[(2\varepsilon k_x+\sigma_x\Delta t).B_x^{n+3/2}\left(i,j+\frac{1}{2},k+\frac{1}{2}\right)\right.$$
$$\left.-(2\varepsilon k_x-\sigma_x\Delta t).B_x^{n+1/2}\left(i,j+\frac{1}{2},k+\frac{1}{2}\right)\right] \quad (2\text{-d})$$

Similar expressions can be derived for the remaining electric and magnetic fields components.

With:

$$\sigma_x(x) = \left(\frac{x}{d}\right)^m . \sigma_{max} \quad (3)$$

$$k_x(x) = 1 + \left(k_{x,max} - 1\right).\left(\frac{x}{d}\right)^m \quad (4)$$

$$\sigma_{max} = -\frac{(m+1)ln\left(R(0)\right)}{2\,\eta\,d} \quad (5)$$

$$R(\theta) = e^{-2\,\eta\,cos\theta\ \int_0^d \sigma(x)\,dx} \text{ (Reflection error)} \quad (6)$$

$$\eta = \sqrt{\frac{\mu}{\varepsilon}} \quad (7)$$

d: The PML area thickness.
x: A positive integer number corresponding to the layer's number $(0 < x < d)$.

Defining the multiplying coefficients of electric and magnetic fields and densities permits a unified treatment of both the interior working volume and the UPML area. The parameters σ and *k* values, in the interior of the working volume, depend on the medium nature. For example in a free space they worth $\sigma = 0$ and $k = 1$. However, in the UPML area the parameters σ and *k* are assumed to have a polynomial-graded profile given by equations (4) and (5).

For computational stability, it is necessary to satisfy the following relation between the space increment Δ*s* and the time increment Δ*t* [7]:

$$\frac{\Delta t}{\sqrt{\mu\varepsilon}} \leq \frac{\Delta s}{\sqrt{3}} \quad (8)$$

In the same context Noda and Yokoyama [14] proposed the following formula to determine the time step Δ*t* :

$$\Delta t = \Delta s \sqrt{\frac{\mu\varepsilon}{3}}(1 - \alpha) \quad (9)$$

α is a small positive value specified by user in order to prevent instability of the numerical integration.

III. LIGHTNING CURRENT AND ELECTROMAGNETIC FIELD COMPUTATION

a. Lightning channel representation

In references [7], [8], [9] and [10], electromagnetic models of lightning return stroke are classified into seven several types depending on lightning return stroke channel representations. These types are a:

1. Perfectly conducting/resistive wire in air above ground;
2. Wire loaded by a additional distributed series inductance in the air above ground;
3. Wire surrounded by a dielectric medium (other than air) that occupies the half space above ground;
4. Wire coated by a dielectric material in the air above ground;
5. Wire coated by a fictitious material having a high relative permittivity and a high relative permeability in the air above ground;
6. two parallel wires having additional distributed shunt capacitance in the air;
7. phase current source array in the air above ground.

Among these seven electromagnetic models we considered, in this work, the second model. This latter consists of a lightning channel considered as a vertical wire loaded by additional distributed series inductance and distributed series resistance. Indeed, this representation is used in order to have a current wave speed lower than the light speed.

Note that this model type has been used by Baba and Rakov in their FDTD computation and analysis of the current distribution along the lightning channel [7], [8], [9] and [10] and by Moini et *al*. in their lightning electromagnetic field calculation based on the use of the moment (MoM) in time domain [5] method.

In figure (1) the return stroke current wire speed along the lightning channel, which is represented by a wire loaded by an additional distributed series inductance, can be calculated using the following relation [9]:

$$v = \sqrt{\frac{L_0}{L_0 + L}}\ c \quad (10)$$

Where *v* is the current wave velocity influenced by the additional inductance *L*.
L_0 is the natural inductance of the vertical wire (L_0=2.1 µH/m [9]), and *c* is the light speed.

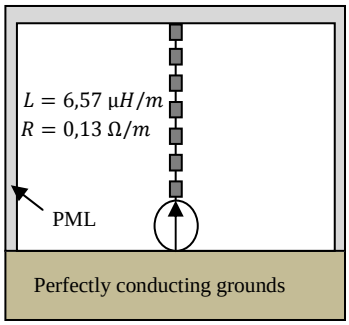

Fig. 1 Lightning return stroke channel represented by a vertical wire loaded by distributed series inductances (*L*=6.57 µH/m) and distributed resistance (R=0,13 Ω/m) above a perfectly conducting ground and excited at its bottom by a current source.

Lightning channel excitation methods used in electromagnetic models can be summarized in four types as following [10]:

1. Closing a charged vertical wire at its bottom with specified impedance.
2. A lumped voltage source.
3. A lumped current source.
4. A phased current source array.

b. Simulation principal

In this work the lightning return stroke channel is represented by a vertical wire placed at the center of a horizontal perfectly conducting plane and excited at its bottom by a current source. The later is represented by an electromagnetic model (Figure (1)).

The study is divided into two parts. In the first one we analyze only the return stroke current distribution along the lightning channel using the electromagnetic model illustrated in Figure (1) and based on the two 3D-FDTD formulations presented before. The second part of this study is reserved to the lightning electromagnetic field components computation. Thus, we compare our results with those computed by Izadi and *al* [12].

In this study, the wire representing the lightning channel has a length of 7.5 km; this length value is close enough to reality since the lightning channel length must not exceed 7.5 km. This wire is placed in a working volume of 90 m x 90 m x 7500 m, which is divided into rectangular parallelepiped cells of 1.5m x 1.5m x 25m. In this way a vertical wire has an equivalent radius of 0.2 m ($r_{eq} = 0.135 \times \Delta x$, according to Taniguchi et *al* [27]). The time increment was fixed to 2 ns.

c. Current time- space distribution along the lightning channel

The vertical wire shown in Figure (1) is excited at its bottom by a lumped current source. This latter produce a current waveform having a peak of 16 kA and a rise time of 0.7 µs. Note that the channel-base current waveform shown at Figure (1) at 0 m is calculated using Heidler function (equation (11)) applied to subsequent return stroke and using parameters illustrated in table 1 and taken from reference [12] for comparison and validation needs.

$$i(0,t) = \frac{i_{01}}{\eta_1}\frac{(t/\tau_{11})^{n_1}}{1+(t/\tau_{11})^{n_1}} exp\left(\frac{-t}{\tau_{12}}\right) + \frac{i_{02}}{\eta_2}\frac{(t/\tau_{21})^{n_2}}{1+(t/\tau_{21})^{n_2}} exp\left(\frac{-t}{\tau_{22}}\right) \quad (11)$$

Where:

i_{01}, i_{02} : are current amplitudes,
τ_{11}, τ_{12} : representing the front time constants,
τ_{21}, τ_{22} : designating the decay time constants,
n_1, n_2 : exponents.

$$\eta_1 = \left[-\left(\frac{\tau_{11}}{\tau_{12}}\right)\left(n_1.\frac{\tau_{12}}{\tau_{11}}\right)^{\frac{1}{n_1}}\right], \quad \eta_2 = \left[-\left(\frac{\tau_{21}}{\tau_{22}}\right)\left(n_2.\frac{\tau_{22}}{\tau_{21}}\right)^{\frac{1}{n_2}}\right]$$

Since, the speed of lightning return stroke current wave is equal to $1.4752.10^8$ m/s [12] (lower than the light velocity), we have taken L = 6.57 µH/m. (calculated using equation (10)).

Table 1. Lightning channel base current parameters

i_{01} (kA)	τ_{11} (µs)	τ_{12} (µs)	i_{01} (kA)	τ_{21} (µs)	τ_{22} (µs)	n_1	n_1
14.8	0.244	2.77	6.86	4.18	40.66	2	2

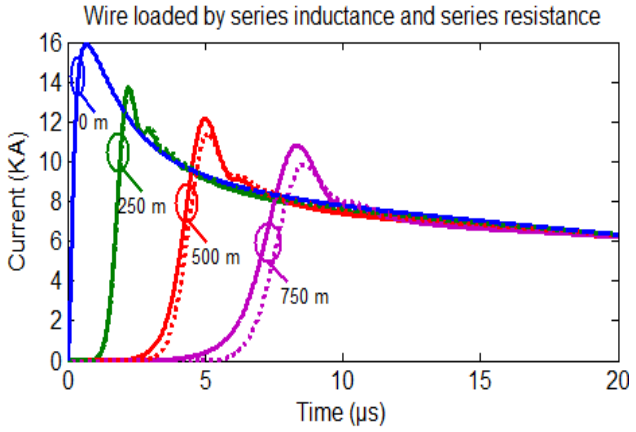

Fig.2 Current waveforms calculated at different heights using 3D-FDTD method and the EM models illustrated in Fig. 1. *Results with dash lines are obtained using Yee algorithm and PEC boundary condition, and those with solid lines are calculated using the Taflove formulation of the 3D-FDTD method and the UPML boundary conditions.*

Thus, in Figure (2) we present a comparison between the current waveforms at different heights namely: 0 m, 250 m, 500 m, and 750 m of the lightning channel. Current waveforms plotted with dash lines are those calculated using Yee algorithm and PEC boundary conditions. Curves plotted with solid lines represent results obtained by the achievement of the 3D-FDTD method and based on Taflove formulation and UMPL boundary conditions. Through this comparison, we can notice the good agreement obtained between the current waveforms for the two approaches notably when the calculation point was locate near the excitation source (at the channel base). However, a significant attenuation in the current distribution magnitudes is observed when this calculation point was far then the current source we have attenuation in magnitudes and difference in time that the current wave take to arrive at the calculation point, so the lightning current wave speed is also affected. These differences remarked on the magnitude and the speed of lightning current wave can be explained by the apparition of reflections of electromagnetic waves and there interaction with source waves when we use PEC boundary conditions, because this later can note avoid all reflection at the work space boundaries, in this effect the UPML boundary conditions are complex in there numerical implementation but are also very effective way used into avoid reflections which can appeared in working volume boundaries.

d. Comparison between simulated and measured Electromagnetic field waveforms

In this section, we compare the electric and magnetic field waveforms, calculated using equations 1-a, 1-b, 2-a, 2-d with similar measurement results taken from reference [12].

Thus, in figure (3) and (4), we present the electromagnetic fields waveforms obtained by simulation and the measured fields collected from a triggered lightning experiment in Florida, USA [12].

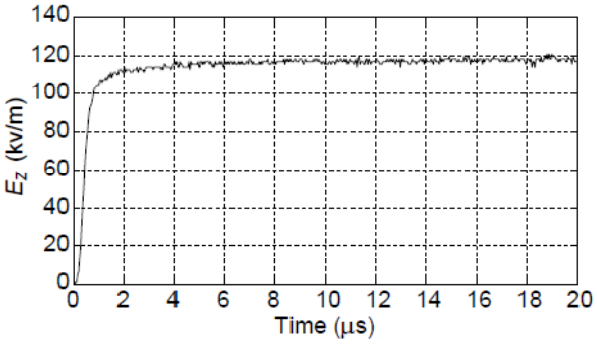

(a)

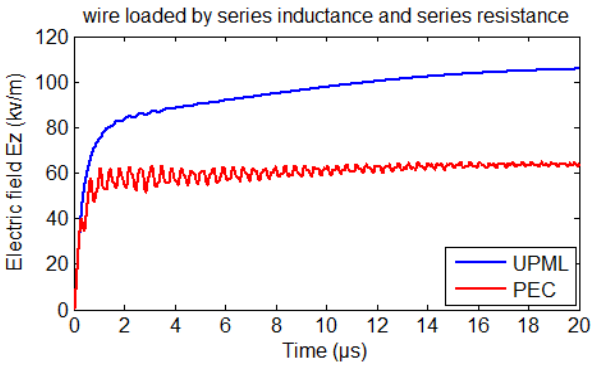

(b)

Fig.3 Calculated and measured vertical electric field waveforms at distance 15 m.
(a) *Measured field [12],* ***(b)*** *3D-FTD calculated field using Yee algorithm combined to PEC boundary conditions and Taflove formulation associated to UPML boundary conditions.*

Figure (3-a) shows the vertical electric field waveforms *measured* at the surface of ground and at distance of 15 m from the lightning channel. In Figure (2-b) we present the vertical electric field waveforms *calculated* using a wire loaded by distributed inductance (L= 6.57 µH/m) and distributed resistance ($R = 0{,}13\ \Omega/m$). Note that results obtained using the Yee algorithm and PEC boundary conditions are drawn in red and those obtained using Taflove formulation and UPML boundary conditions are drawn in blue. It can be observed that the waveform calculated using Taflove formulation of 3D-FDTD method and UPML boundary condition is more damped than the one obtained using Yee algorithm and PEC boundary conditions. Indeed, oscillations appear on this later and the magnitude attenuation is caused by lighting electromagnetic waves reflections. These vertical electric field deformations are due to the PEC boundary conditions use. Finally, we can also notice a satisfactory agreement between the calculated electric field (using the 3D-FDTD method and UMPL boundary conditions) and the measured one. However, the observed differences between the calculated and measured results can be attributed to many factors such as: measurement device errors, miscalculations due to the vertical lightning channel assumption, lightning return stroke speed change which has not been considered in the calculation, and the ground conductivity which has a finite value.

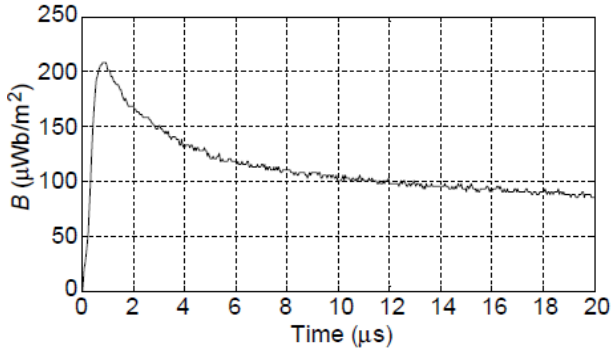

(a)

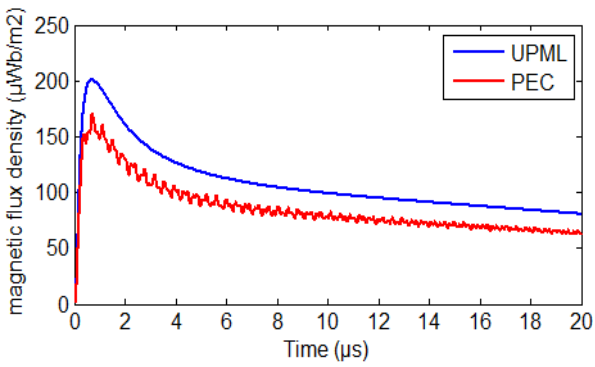

(b)

Fig.4 Calculated and measured magnetic flux densities waveforms at distance 15 m.
(a) *Measured waveform [12],* ***(b)*** *3D-FTD calculated waveform using Yee algorithm combined to PEC boundary conditions and Taflove formulation associated to UPML boundary conditions*

Figure (4) shows calculated and measured, magnetic flux density waveforms, at distance of 15 m from the lightning channel. The magnetic flux density measured at distance of 15 m from the lightning channel taken from reference [12] is presented in Figure (4-a). In figure (4-b) we present magnetic flux density calculated using Yee algorithm with PEC boundary conditions (dawn in red), and the new approach based on the implementation of Taflove formulation in the 3D-FDTD method with UPML boundary conditions (drawn in blue). There also we observe that the new approach waveform is more damped then that one obtained by using Yee algorithm and PEC boundary conditions. A good agreement is also shown between the calculated waveform based on the new approach and the measured one. The waveform obtained using Yee algorithm and PEC boundary conditions is characterized by a magnitude attenuation and appearing of oscillations caused by lightning electromagnetic waves reflections in the working space boundaries.

IV. CONCLUSION

The new approach proposed in this paper, based on the use of Taflove formulation in the 3D-FDTD method associated to the UPML boundary conditions to calculate the electromagnetic field associated to the lightning return stroke current was implemented in a 3D computing code developed in Matlab environment and validated by comparison of the

obtained results with measured data. The lightning return stroke current distribution used in the electromagnetic field computation was evaluated by the achievement of an electromagnetic model.

ACKNOWLEDGMENT

Part of this study was realized in the Power System Analysis Laboratory (PSAL) of Doshisha University-Japan. The authors would like to thank Prof. Y. Baba for his useful comment and help, and Pof. A. Amitani, Prof. N. Nagaoka and Dr. T. H. Thang for their kind cooperation.

REFERNECES

[1] V. A. Rakov, and M. A. Uman, "Review and evaluation of lightning return stroke models including some aspects of their application", IEEE Trans. Electromagnetic Compatibility. Vol. 40, NO. 4, Nov. 1998.

[2] M.Van Baricum and E. K. Mailler, "TDWTD — A Computer Program for Time-Domain Analysis of Thin-Wire Structures", Livermore. CA: Lawrence Livemore Lab. 1972.

[3] R. F. Harrington, "Field Computation by Moment Methods", New York: Macmillan, 1968.

[4] K. S. YEE "Numerical solution of initial boundary value problems involving Maxwell's equations in isotropic media", IEEE Trans. Antennas and Propagation. Vol. AP-14, NO 3 pp 302-307, May, 1966.

[5] R.Moini, B. Kordi, G. Z. Rafi,and V. A. Rakov," A new lightning return stroke model based on antenna theory ", Journal of geophysical research, Vol. 105, NO. D24, pages 29,693 – 29,702, December 27, 2000.

[6] A. Shoory, R. Moini, S. H. H. Sadeghi, and V. A. Rakove, " Analysis of lightning radiated electromagnetic fields in vicinity of lossy ground", IEEE Tans. Electromagnetic Compatibility, vol, 47, no. 1, pp 131-145, Feb. 2005.

[7] Y. Baba and V. A. Rakov "Application of electromagnetic models of the lightning return stroke", IEEE Trans. Power Delivery. Vol. 23, NO. 2, April 2008.

[8] Y. Baba and V. A. Rakov "Electric and magnetic fields predicted by different electromagnetic models of the lightning return stroke versus measurement", IEEE Trans. Electromagnetic Compatibility. Vol. 51, NO. 3, August 2009.

[9] Y. Baba and V. A. Rakov "Electromagnetic models of the lightning return stroke", Journal of Geophysical research. Vol. 112, 2007.

[10] Y. Baba and V. A. Rakov "Application of the FDTD method to lightning electromagnetic pulse and surge simulation", IEEE Trans. Electromagnetic Compatibility. Vol. 56, NO. 6, Dec. 2014.

[11] A. Taflove, and S. C. Hagness, "Computational Electrodynamics: The Finite-Difference Time-Domain method", Second Edition, Artech House, Boston-London, 2000.

[12] M. Izadi, M. Z. A. AbKadir, C. Gomes, and V. Cooray " Evaluation of lightning return stroke current using measured electromagnetic fields", Progress In Electromagnetic Research, Vol, 130, 581-600, 2012.

[13] J. P. Berenger, "Three-dimensional perfectly matched layer for the absorption of electromagnetic waves", Journal of Computational Physics. 127, pp 363-379, 1996.

[14] T. Noda and S. Yokoyama "Thin wire representation in finite difference time domain surge simulation", IEEE Trans. Power Delivery. Vol. 17, NO. 3, July 2002.

[15] Y. Taniguchi, Y. Baba, N. Nagaoka and A. Amitani "An improvement of thin wire representation for FDTD Electromagnetic and surge calculations", IEEE Trans. Antennas and propagation. Vol. 56, issu:10, pp 3248 – 3252, oct 2008.

[16] A. Amitani, N. Nagaoka, Y. Baba and T. Ohno, "Power System Transients – Theory and Applications", CRC Press. Taylor and Francis group, 2014.

[17] Y. Baba and V. A. Rakov "On the use of lumped sources in lightning return stroke models", Journal of Geophysical research. Vol. 110, D03101, 2005.

[18] Y. Baba and V. A. Rakov "On the transmission line model for lightning return stroke representation", Geophysical research Letters. Vol. 30, NO. 24, 2003.

[19] Y. Baba and V. A. Rakov "Evaluation of lightning return stroke electromagnetic models", 29th International Conference on Lightning protection.23rd – 26th June 2008 – Uppsala, Sweden.

[20] Y. Baba and V. A. Rakov "On the mechanism of attenuation of current waves propagating along a vertical perfectly conducting wire above ground: Application to lightning", IEEE Trans. Electromagnetic Compatibility Vol. 47, NO. 3, August 2005.

[21] Y. Baba and V. A. Rakov "Characteristics of electromagnetic return-stroke models", IEEE Trans. Electromagnetic Compatibility. Vol. 45, NO. 1, Feb. 2003.

[22] M. N. O. Sadiku, "Numerical techniques in electromagnetic", CRC Press. Boca Raton New York Washington, D.C 2000.

[23] D. M. Sullivan, "Electromagnetic simulation using the FDTD method", IEEE Press series on RF microwave technology, 2000.

[24] M. M. F. Saba, O. Pinto Jr., and M. G. Ballarotti,"Relation between lightning stroke peak current and following current", *Geophysical research Letters.* Vol. 33, 2006.

[25] T. H. Tahang, Y. Baba A. Amitani, and V. Rakov "FDTD simulation of corona effect on lightning-induced voltages", IEEE Trans. Electromagnetic Compatibility. Vol. 56, NO. 1,Fev. 2014.

[26] H. Oka, Y. Baba, M. Ishii, N. Nagaoka, and A. Amitani "Parametric Study on unit step responses of impulse voltage measuring systems based on FDTD simulations", IEEE Trans. Power Delivery Vol. 28, NO. 1,Fev. 2013.

[27] Y. Taniguchi, Y. Baba, N. Nagaoka and A. Amitani "Modification on thin wire representation for FDTD calculations in nonsquare grids", IEEE Trans. Electromagnetic Compatibility. Vol. 50, pp 427 – 431, May 2008.